

UC Irvine

UC Irvine Previously Published Works

Title

A two-step method for identifying photopigment opsin and *rhodopsin* gene sequences underlying human color vision phenotypes.

Permalink

<https://escholarship.org/uc/item/0nf210rs>

Authors

Atilano, Shari R
Kenney, M Cristina
Briscoe, Adriana D
et al.

Publication Date

2020

Peer reviewed

A two-step method for identifying photopigment opsin and rhodopsin gene sequences underlying human color vision phenotypes

Shari R. Atilano,¹ M. Cristina Kenney,^{1,2} Adriana D. Briscoe,³ Kimberly A. Jameson⁴

¹Gavin Herbert Eye Institute, School of Medicine, University of California, Irvine, CA; ²Department of Pathology and Laboratory Medicine, University of California Irvine, Irvine, CA; ³Department of Ecology and Evolutionary Biology, University of California Irvine, Irvine, CA; ⁴Institute for Mathematical Behavioral Sciences, University of California Irvine, Irvine, CA

Purpose: To present a detailed, reliable long range-PCR and sequencing (LR-PCR-Seq) procedure to identify human opsin gene sequences for variations in the long wavelength-sensitive (*OPN1LW*), medium wavelength-sensitive (*OPN1MW*), short wavelength-sensitive (*OPN1SW*), and rhodopsin (*RHO*) genes.

Methods: Color vision was assessed for nine subjects using the Farnsworth-Munsell 100 hue test, Ishihara pseudo-isochromatic plates, and the Rabin cone-contrast threshold procedure (ColorDX, Konan Medical). The color vision phenotypes were normal trichromacy (n = 3), potential tetrachromacy (n = 3), dichromacy (n = 2), and unexplained low color vision (n = 1). DNA was isolated from blood or saliva and LR-PCR amplified into individual products: *OPN1LW* (4,045 bp), *OPN1MW* (4,045 bp), *OPN1SW* (3,326 bp), and *RHO* (6,715 bp). Each product was sequenced using specific internal primer sets. Analysis was performed with Mutation Surveyor software.

Results: The LR-PCR-Seq technique identified known single nucleotide polymorphisms (SNPs) in *OPN1LW* and *OPN1MW* gene codons (180, 230, 233, 277, and 285), as well as those for lesser studied codons (174, 178, 236, 274, 279, 298 and 309) in the *OPN1LW* and *OPN1MW* genes. Additionally, six SNP variants in the *OPN1MW* and *OPN1LW* genes not previously reported in the NCBI dbSNP database were identified. An unreported poly-T region within intron 5(c.36+126) of the *rhodopsin* gene was also found, and analysis showed it to be highly conserved in mammalian species.

Conclusions: This LR-PCR-Seq procedure (single PCR reaction per gene followed by sequencing) can identify exonic and intronic SNP variants in *OPN1LW*, *OPN1MW*, *OPN1SW*, and *rhodopsin* genes. There is no need for restriction enzyme digestion or multiple PCR steps that can introduce errors. Future studies will combine the LR-PCR-Seq with perceptual behavior measures, allowing for accurate correlations between opsin genotypes, retinal photopigment phenotypes, and color perception behaviors.

Across normal individual visual systems, the photo-sensitive layers of the retina are highly variable in structure and function. Two photopigments are coded from the X-chromosome (*OPN1LW*- Gene ID: 5956 OMIM: [300822](#) and *OPN1MW* -Gene ID: 2652 OMIM: [300821](#) [Table 1]) while the *OPN1SW* (Gene ID: 611 OMIM: [613522](#)) is on chromosome 7q32.1, and *rhodopsin* (Gene ID: 6010 OMIM: [1803800](#)) is from chromosome 3q22.1. Human genotype or perceptual-phenotype analyses show that genotypic variation corresponds to shifts in the absorption spectra of expressed retinal photopigments [1-4] with concomitant shifts in peak perceptual spectral sensitivity to light, or “λ-max,” in human subjects [5-7]. There is increasing interest in correlating the opsin genotypes with the color perception phenotypes in patients with age-related retinal diseases, but the complexity of the opsin genes has made this task difficult.

The greatest variations in color perception are due to codon changes in the long-wavelength and medium-wavelength opsin genes. The average ratio of long-wavelength to middle-wavelength (L:M) cone photoreceptors in normal color vision is estimated at 2.5:1.0, but this cone ratio can range from 1.1:1.0 to 16.5:1.00 [8,9]. The *OPN1LW* and *OPN1MW* opsin exon gene sequences are 96% homologous and differ at only seven locations where important amino acid substitutions occur. It has been shown that *OPN1LW* and *OPN1MW* single amino-acid substitutions at codon 180 in exon 3 and codons 277 and 285 in exon 5 produce large shifts in spectral sensitivity, whereas substitutions at codons 230 and 233 in exon 4 produce smaller shifts [1,2,10]. Substitutions of amino acid residues at key positions are associated with predictable shifts in λ-max in various mammalian species. Mammals whose *OPN1LW* and *OPN1MW* genes demonstrate codon conservation at these key residues include cat, guinea pig, rabbit, dolphin, mouse, rat, and several species of New World monkeys [11-13]. The “three-sites” amino acid composition (180, 277, and 285) in the L/M opsins dictate the λ-max values

Correspondence to: Kimberly Jameson, IMBS, Social Science Plaza, UC Irvine, Irvine, CA, 92697-5100; Phone: (949) 824-8651; FAX: (949) 824-3733; email: kjameson@uci.edu

TABLE 1. DESCRIPTION OF OPSIN GENES.

Symbol (Gene ID)	Gene name	Cell type	Chromosome	Reference sequences: Genomic mRNA protein
OPN1LW (5956)	<i>Homo sapiens</i> opsin 1 (cone pigments), long-wave-sensitive	Red cone	Xq28	NG_009105.2 NM_020061.5 NP_064445.2
OPN1MW (2652)	<i>Homo sapiens</i> opsin 1 (cone pigments), medium-wave-sensitive	Green cone	Xq28	NG_011606.1 NM_000513.2 NP_000504.1
OPN1SW (611)	<i>Homo sapiens</i> opsin 1 (cone pigments), short-wave-sensitive	Blue cone	7q32.1	NG_009094.1 NM_001708.2 NP_01699.1
RHO (6010)	<i>Homo sapiens</i> rhodopsin	Rod	3q22.1	NG_009115.1 NM_000539.3 NP_000530.1
EXON 5 - OPN1LW and OPN1MW	Exon 5 of OPN1LW and OPN1MW	N/A	Xq28	NG_009105.2 NM_020061.5 NG_011606.1 NM_000513.2

for humans along with species of New World and Old World monkeys [14]. Identifying genetic sequence variations is important to understand the ranges of normal and deficient color vision phenotypes.

Extensive DNA sequence homology between *OPN1LW* and *OPN1MW* has historically presented challenges for sequence differentiation when conventional PCR is used, and such difficulties are further compounded when investigations require study of large numbers of subjects. Previously, this challenge was addressed by Neitz and coworkers, who reported methods using two real-time PCR assays to generate an exon 5 product, which can be further amplified using exon-specific primers [15]. One advantage of the Neitz et al. (2004) technique is that the exon amplification includes the intron or exon junctions [15], and subsequently, it has been adopted by other laboratories [16,17]. A disadvantage of the Neitz et al. (2004) technique is that multiple PCR assays are required for each specimen analyzed, which increases risks of genotyping analysis errors, as well as monetary costs. Alternatively, Gardner and coworkers presented a modified Michaelides et al. approach to analyze three families for blue cone monochromatism using PCR to coamplify the locus

control region (upstream of the L-opsin gene) along with six exons of the L- and M-opsin genes [18,19]. After sequencing with internal primers, the L- versus M-opsin exons 2–5 could be distinguished. However, applying the Michaelides et al. technique to large numbers of subjects remains costly and is cumbersome [18]. In comparison, Oda et al. characterized 63 Japanese subjects using a different methodology that involved PCR, followed by gel purification and single-strand conformation polymorphism analyses [20], a technique combined with direct sequencing to detect viroid DNA polymorphisms and point mutations [21–24]. Jameson and coworkers developed a multistep technique for identifying the single nucleotide polymorphisms (SNPs) in the *OPN1LW* and *OPN1MW* genes [25,26]. Their technique involved long-range PCR of the L- and M-opsin genes, followed by PCR and sequencing of exon 4. An additional step involved PCR and restriction enzyme digestion of exon 3 to identify the codon 180 configuration in the *OPN1LW* versus *OPN1MW* genes. The disadvantages of these methods are the following: (a) time-consuming with multiple steps; (b) expensive; (c) high potential for errors due to restriction fragment length polymorphism (RFLP) inefficiencies, especially when analyzing exon 3; (d) limited to finding mutations or SNP variants only

within the short-range PCR products, which leaves large expanses unexamined; and (e) cumbersome for analyzing large populations (more than 100 subjects).

More recently, Davidoff and coworkers employed a MassArray system in which a short sequence region was amplified around known target SNP areas of genomic DNA. The region examined was then further modified and analyzed with matrix-assisted laser desorption/ionization-time-of-flight (MALDI-TOF) mass spectrometry, permitting simultaneous identification of multiple SNPs [27]. With this technique, codons 116, 180, 230, and 309 and a promoter region SNP (p1) could be identified in a large sample, making this technique a good screening test. However, a disadvantage of this technique is that unknown or novel SNP mutations or variants might be missed because the process does not sequence entire opsin genes.

The present study presents a reliable, uniform method that can be applied to all opsin genes. This approach utilizes long-range (LR) PCR to amplify products that range in size from 3,326 to 6,715 bp (Table 2). Sequencing of each LR-PCR product then uses three to four internal sequencing primers for the *long*, *medium*, and *short opsin* and *rhodopsin* genes. Because exon 5 is important, it underwent an additional PCR to yield a 398 bp product that was sequenced separately. The advantages of this method are as follows: (a) Using a uniform method, large numbers of subjects (>100) can be analyzed for variants in the introns and exons of the *short*, *medium*, and *long opsin* and *rhodopsin* genes; (b) there are fewer steps (a single PCR followed by sequencing), so fewer chances for errors; (c) no restriction enzyme digestion is required; (d) the procedures are cost effective; and (e) the yield and amplification specificity, especially for G-C rich and secondary structure, are improved because of the use of high-fidelity FailSafe polymerase (Middletown, WI) that contains betaine/trimethyl glycine as a PCR enhancer [28-30].

The final goal for this study was to provide step-by-step protocols, including primer sequences and PCR program parameters for opsin genotyping so that the procedures can be adopted in multiple laboratories. If successful, increased usage of this uniform technique for opsin genotyping should allow for ease of identifying and characterizing genetic sequence variations to be correlated with perceptual behaviors commonly seen among individuals of established retinal phenotypes.

METHODS

Subjects: This study adhered to the principles of the World Medical Association Declaration of Helsinki, the highest level of ethical conduct when using human subjects per

The Association of Research in Vision and Ophthalmology (ARVO) policies, and was approved by the Institutional Review Board of the University of California, Irvine (IRB #2003-3131). All subjects read and signed an informed consent. Nine subjects were selected with the express purpose of sequencing opsin genotypes from individuals with superior, average, or poor color vision discrimination (Table 3). The nine subjects were specifically selected to span a range of retinal processing phenotypes, which can be classified into three groups to illustrate relationships between these genotyping methods and color vision phenotypes as measured with standardized color perception tests. The three color perception groups were (i) male and female subjects with normal trichromat color vision who were expected to have normal trichromat color vision genotypes ($n = 3$); (ii) female subjects with known color perception anomalies in male family members, who exhibited normal trichromat color vision on standardized tests, but who were expected to have potential tetrachromat color vision genotypes ($n = 3$); (iii) male subjects with abnormal color vision on standardized color perception tests, who were classified perceptually as dichromats ($n = 2$), as well as one individual exhibiting low color vision performance ($n = 1$). Thus, subjects from the last group were expected to have some form of allelic variation, or genetic sequence anomaly, identified in their color vision opsin genotype results. The purpose of assessing this variety of nine subjects was twofold: first, to illustrate that the present genotyping procedures can successfully identify gene sequences that are known to consistently vary across a range of opsin genotypes, and second, that the genotypes identified for each of the nine subjects is compatible with a color vision phenotype classification suggested by the subjects' color perception results as found with standard color vision assessment procedures.

Color vision assessment procedures: Each subject's ($n = 9$) color perception was tested with three standardized procedures using the Ishihara pseudoisochromatic plates (Ishihara S. Tokyo, Japan: Kanehara & Co., Ltd 1994), the Farnsworth-Munsell 100 hue (FM100) color vision test [31,32], and Konan Medical's implementation of the Rabin cone-contrast threshold procedure, referred to below as the "ColorDx" assessment method [33,34]. Subjects' Rabin cone-contrast thresholds were assessed for achromatic acuity and independently for S-, M-, and L-cone chromatic contrast in lieu of the typically assessed (albeit arguably less informative) anomaloscope Rayleigh match ranges. All subjects had 20/20 Snellen or better binocularly corrected visual acuity.

Color vision assessment required individuals to complete between 1.0 and 2.5 h of participation using standardized tools

TABLE 2. OPSIN PRIMERS FOR PCR AND SEQUENCING.

Symbol	Primer F	Primer R	Internal sequencing primers	Product size (bp)
			PRIMERS	
OPN1LW ^a	GGCAACATAGTGAGACCTCTTCTC	CCAGCAGACGCAGTACGCAAGAT	E3F: CTCAGTCCGTGGAGCCCTGAATTC E4F: ACAAAACCCACCCGAGTTAG E4R: GACTCATTTGAGGGCAGAGC	4045
OPN1MW ^b	GGCAACATAGTGAGACCTCTTCTC	CCAGCAGAACGAGAAATGCCAGGAC	E3F: CTCAGTCCGTGGAGCCCTGAATTC E4F: ACAAAACCCACCCGAGTTAG E4R: GACTCATTTGAGGGCAGAGC	4045
OPN1SW ^b	AAGAGGACTCAGAGGGGGGTGTG	AAAATTAAATTCTAGCTGTTGCAAAC	E2F: GCCATTATCCTCACATTTCACC E3F: GGAGAACACAAATCCAGGCATCT E4F: GATGTGATGCTTTCCGTGCT	3326
RHO ^c	TCAGAACCCAGAGTCATCCA	CCTACTGTGTGCCCCATTCT	E1R: GGACAGGAGAGGGGAGAAGG E2R: CCAGCCCTGTAGCAACATT E3_4R: ACTGCTGACCCCAAGACTGCT E5F: AGCTGGATTTGAGTGGATGG	6715
EXON 5 - OPN1LW and OPN1MW ^d	CTATGCCTGGGTACCTGCCTC	CTTATCAGAGACATGATTCCAGGTGG	N/A	398

^aJameson Technical Report Series # MBS 09-07: Long-Range Polymerase Chain Reaction Method for Detection of Human Red and Green Opsin Gene Polymorphisms^b Baraas et al. 2012 and Gunther et al. 2006 **modified primers ^c Kim et al. *Molecular Vision* 2011; 17:844-853 Spectrum of rhodopsin mutations in Korean patients with retinitis pigmentosa ^d McClements et al. IOVS Feb 2013 Vol 54 No2

TABLE 3. SUBJECT DEMOGRAPHICS AND COLOR VISION ASSESSMENT.

Subject	Age	Sex	Self Identified Race/Ethnicity	14 Ishihara Plates Performance	FM100 Color Vision Diagnosis (Farnsworth Munsell 100 Hue Test)	FM100 Total Error Score	ColorDX S/M/L Performance
1	53	F	Multi	No errors	Superior	16	Pass/Pass/Pass
2	20	F	Asian	No errors	Superior	12	Pass/Pass/Pass
3	26	F	Asian	No errors	Superior	12	Pass/Pass/Pass
4	61	M	White	No errors	Average	20	Pass/Pass/Pass
5	60	F	White	No errors	Average	20	Pass/Pass/Pass
6	41	F	Multi	No errors	Average	32	Pass/Pass/Pass
7	90	M	White	No errors	Low Trichromat discrimination	120	Low/Low/Low
8	32	M	White	12 errors	Strong Deutan deficiency	356	Pass/Fail/Low
9	41	M	Hispanic	11 errors	Strong Protan deficiency	160	Pass/Low/Fail

NOTE. Subject 7 exhibits color vision assessment performance on all tests that are consistent with age-related norms for normal color vision trichromats. Subject 8 exhibits color vision assessment performance consistent with Deuteranopia, or M-cone deficiency. Subject 9 exhibits color vision assessment performance consistent with Protanopia, or L-cone deficiency.

and methods. In preparation for the color vision assessment, subjects were visually adapted in an otherwise neutral achromatic viewing booth for 15 min to a full-spectrum (5,000 K) daylight-approximate illuminant designed for industrial color proofing (GTI GLL-440, Middleton, WI; 4-Lamp Luminaire). The GTI daylight approximate light source was used to illuminate the Ishihara pseudoisochromatic plates and the Farnsworth-Munsell 100 hue test, which were administered using standard procedures under binocular viewing once the adaptation interval was completed.

Following the Ishihara pseudoisochromatic plates and the FM100 test, subjects were subsequently adapted for 15 min to a low-light ambient environment (approximately 5 lux) in preparation for the ColorDx binocular cone-contrast threshold assessment using robust Psi marginal threshold-setting procedures [35] on a calibrated computer display and a neutral gray adaptation surround (see ColorDx). All nine subjects completed the color contrast threshold setting portion of the ColorDx assessment within 30 min. A 15-min debriefing completed the perceptual portion of the testing session. All nine subjects completed all portions of the color vision assessment.

DNA extraction methods: DNA was isolated from four subjects from 10 ml of peripheral blood leukocytes using a DNA isolation kit (PureGene, Qiagen, Valencia, CA) according to the manufacturer's protocol. DNA was also isolated from saliva (n = 5) using a kit (Oragene-DISCOVER kit, DNA Genotek Inc., Ottawa, Canada) according to the manufacturer's protocol. The present genotyping procedures were found to perform consistently for DNA collection

methods (blood and saliva), and for a subset of subjects both were used. All comparisons of the genotype results were confirmed across specimens.

Long-range PCR for sequencing (LR-PCR-Seq): All PCRs were performed with 100 ng DNA with a PCR System (FailSafe PCR System-Buffer D, Lucigen, Middleton, WI) according to the manufacturer's protocol. The FailSafe PCR Enzyme Mix is a unique blend of thermostable DNA polymerases containing a 3' to 5' proofreading enzyme for high fidelity with a premix containing a buffered salt solution with all four dNTPs, various amounts of MgCl₂, and FailSafe PCR Enhancer (with betaine). The system has high PCR accuracy with a threefold lower error rate (1 in 30,000 bases) than *Taq* DNA polymerase. Table 1 describes the chromosomal location for the *OPN1LW*, *OPN1MW*, *OPN1SW*, and *RHO* genes. The primers and the product sizes for each of the opsin genes and exon 5 are described in Table 2. Potential primer mismatch was checked by UCSC In-Silico PCR (Genome) and/or NCBI, and none was found.

The PCR program for *OPN1LW* and *OPN1MW* was initial denaturation at 90 °C for 2 min, 35 cycles of 90 °C for 10 s, 68 °C for 4 min and 30 s with a final extension at 72 °C for 10 min. The PCR program for *OPN1SW* was initial denaturation at 94 °C for 5 min, 35 cycles of 95 °C for 45 s, 56 °C for 45 s, 72 °C for 3 min and 30 s with a final extension at 72 °C for 7 min. The PCR program for *RHO* was initial denaturation at 94 °C for 5 min, 35 cycles of 95 °C for 45 s, 58 °C for 45 s, 72 °C for 5 min and 30 s.

Exon 5 for the *OPN1LW* and *OPN1MW* genes was sequenced to help verify the presence of both genes, which

have unique variations in this region [26]. The PCR program for exon 5 of *OPN1LW* or *OPN1MW* was initial denaturation at 95 °C for 1 min, 35 cycles of 95 °C for 30 s, 58 °C for 30 s, 72 °C for 30 s with a final extension at 72 °C for 10 min. All PCR products were visualized on 1% agarose gels (Figure 1; E-gel 48, Mother E-base, ThermoFisher, Huntington Beach, CA). Figure 2 provides in-depth information used to distinguish between the *OPN1LW* and *OPN1MW* genes, including the gene-specific sequences within exon 5. The specific LR-PCR-Seq products showing unique amino acids and DNA bases for the long versus medium opsin genes are bolded. Within exon 5 of both genes, there are seven nucleotide differences that yield seven different amino acids (274I/V, 275F/L, 277Y/F, 279V/F, 285T/A, 298A/P, and 309Y/F).

In preparation for sequencing, PCR products were treated with an Exonuclease I and Shrimp Alkaline Phosphatase formulation (ExoSAP-IT, ThermoFisher) according to the manufacturer’s protocol. Sanger sequencing was

performed at ELIM BioPharm (Hayward, CA) using internal primers (Table 2, Appendix 1). Analyses were conducted with sequencing software (Mutation Surveyor, SoftGenetics, State College, PA).

RESULTS

LR-PCR-Seq analyses: The nine subjects illustrate informative relationships between genotyping results and color vision discrimination behaviors. The LR-PCR-Seq results are shown for the *OPN1LW*, *OPN1MW*, *OPN1SW*, and *RHO* (Appendix 2) genes. Appendix 2 summarizes the distribution of 12 commonly recognized SNP changes in the *OPN1LW* gene that yielded amino acid changes in the nine subjects. For example, SNP 13737A>C (rs713; Met152Leu) was found in subjects 1, 2, 3, 4, 5, 6, and 7 but not in subjects 8 and 9. Two of the variants ([rs149897670](#), Ala174Val and rs145009674, Ile178Val) were not found in the nine subjects we analyzed.

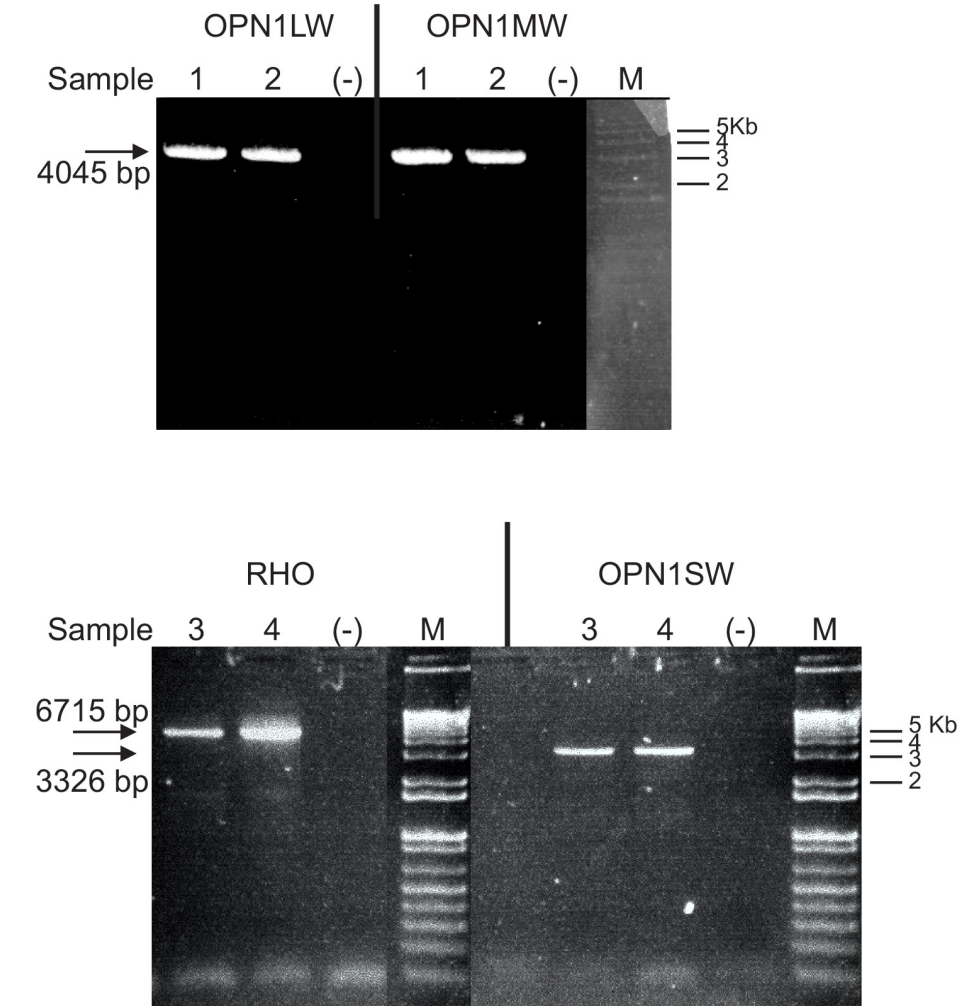


Figure 1. Representative gel images of *OPN1LW*, *OPN1MW*, *RHO*, and *OPN1SW* PCR products. The first gel image represents the PCR products of *OPN1LW* and *OPN1MW* from two subjects. The size of both PCR products is 4,045 bp. M = DNA ladder. The DNA ladder positions are identified at 5, 4, 3, and 2 kb. The second gel image represents the PCR products of *RHO* and *OPN1SW* in subjects 3 and 4. The *RHO* PCR product is 6,715 bp. The *OPN1SW* PCR product is 3,326 bp.

Ref LW/MW	Exon 5 (codon 249)	V A K Q Q K E S E S T Q K A E K E V T R M V V V M I/V
Ref LW		cactatccctgtctcccttaggtggcaagcagcagaaagagtctgaatccacccagaaggcagagaaggaagtgacgcgcgatggtggtgatgat atct
Ref MW		cactatccctgtctcccttaggtggcaagcagcagaaagagtctgaatccacccagaaggcagagaaggaagtgacgcgcgatggtggtgatgat gtcc
Ref LW		F/L A Y/F C V/F C W G P Y T/A F F A C F A A A N P G Y A/P F H P L M A A L P A
Ref LW		<u>ttgcgtactgcgtctgctggggaccctac</u> accttcttcgcgatgctttgctgctgccaaccctgggtac gccttccaccctttgatggctgcctgcccggc
Ref MW		<u>tgccattctgcttctgctggggaccatac</u> gccttcttcgcgatgctttgctgctgccaaccctgggtac cccttccaccctttgatggctgcctgcccggc
		*Reverse Primer
		Y/F F A K S A T I Y N P V I Y V F M N R Q
Ref LW		ctactttgcaaaagtgcactatctacaaccccggttatctatgtctttatgaaccggcaggtaagcaacaccatcagcagatcccaactcaaaataccgt
Ref MW		cttctttgcaaaagtgcactatctacaaccccggttatctatgtctttatgaaccggcaggtaagcaacaccatcagcagatcccaactcaaaataccgt

Figure 2. Schematic comparing the nucleotide sequences and amino acid profile of the *OPNILW* and *OPNIMW* genes. The different sites are codon 274 I/V, codon 275 F/L, codon 277 Y/F, codon 279 V/F, codon 285 T/A, codon 298 A/P, and codon 309 Y/F.

Representative chromatograms in the region of *OPNILW* codon 180 (rs949431) are shown in Figure 3. Codon 180 of exon 3 is common and known to affect wavelength sensitivity, and therefore, has been the focus of many studies [10,36]. Subjects 5, 7, and 8 had homozygous GG nucleotides at the 180 position (Alanine; Appendix 2). Subjects 1, 3, 4, and 6 were heterozygous GT (180Ala/Ser). Subject 2 was homozygous TT (180Ser). The *OPNILW* codon 180 in subject 8 was GG/180Ala. We could not generate an *OPNILW* PCR product for subject 9 despite multiple PCR attempts. We hypothesized that subject 9 had a hybrid *OPNILW* gene in which exon5 of *OPNILW* had been replaced by exon 5 of *OPNIMW*. Thus, the *OPNILW* reverse primer could not anneal at the expected location, and the PCR failed. This was supported by the subsequent analysis of exon 5 in subject 9 that did not show the expected heterozygosity of the combined *OPNILW* and *OPNIMW* PCR product but showed the homozygous sequence of only *OPNIMW* exon 5. The SNP 17119A>G was identified in the Genomic Reference database but has not been assigned a reference sequence, or “rs,” number. The information included in the Appendix 1 shows additional SNPs that can be identified with the LR-PCR-Seq technique.

The LR-PCR-Seq analyses for the *OPNIMW* gene identified all the common codons (180, 230, 233, 277, and 285; Appendix 2). However, in addition, less frequently studied codons (174, 178, 236, 274, 279, 298, and 309) were identified with this technique, demonstrating the large amount of information that can be gathered in a single sequencing step. For subject 8, the *OPNIMW* PCR was unsuccessful, mostly likely due to the failure of the *OPNIMW* reverse primer to anneal. This was supported by sequencing of exon 5 in subject 8 which was homozygous for *OPNILW* nucleotides indicating a missing exon 5 in *OPNIMW*.

Appendix 2 shows the SNPs identified in the *OPNISW* gene are either intronic variants or synonymous substitutions

(p.Gly122). LR-PCR-Seq of the *RHO* gene yielded ten different SNP variants (Appendix 2), all having rs numbers, which is not surprising because the *rhodopsin* gene has been the most investigated of the *opsin* genes.

Poly-T region of rhodopsin: When the *rhodopsin* gene (NG_009115) was analyzed using the LR-PCR-Seq method, there was some sequencing slippage within intron 5. Additional analyses determined that a previously unreported poly-T region was present near the terminus of exon 5 (c.36+126; Figure 4A). Forward and reverse primers (5F and 5R) are required to completely sequence the exon. The intron 5 poly-T variation was verified using whole genome next-generation sequencing (HiSeq, Illumina, San Diego, CA) of blood DNA (data not shown).

This poly-T region within intron 5 (c.36+126) ranged from 14 to 16 nucleotides and was consistently found in the nine subjects (Figure 4B). Due to this consistent finding, we wanted to determine whether this poly-T site was conserved in other species. Investigation of 18 different species showed the conserved nature of the poly-T sites (Figure 4C). The shortest poly-T sequence was ten poly-T sites (*Pan paniscus*), while the longest (16 poly-T sites) was in *Homo sapiens*, *Ptilio-colobus Tephrosceles*, and *Chlorocebus sabaeus*. The significance of this poly-T sequence is not clear, but laboratories that use the LR-PCR-Seq method should be aware of its presence when analyzing the sequencing data.

Correlation of color vision assessment and genotype: The color vision assessments (Table 3) can be correlated with the photopigment opsin genotype obtained using LR-PCR-Seq (Appendix 2). Ideally for opsin genotyping to be useful as a tool for investigating perceptual and clinical variations in color processing, it should provide easily interpreted genotyping analyses, and consistently correspond to color vision assessments. For example, a subject who is identified by the present genotyping procedures as lacking *OPNIMW* or

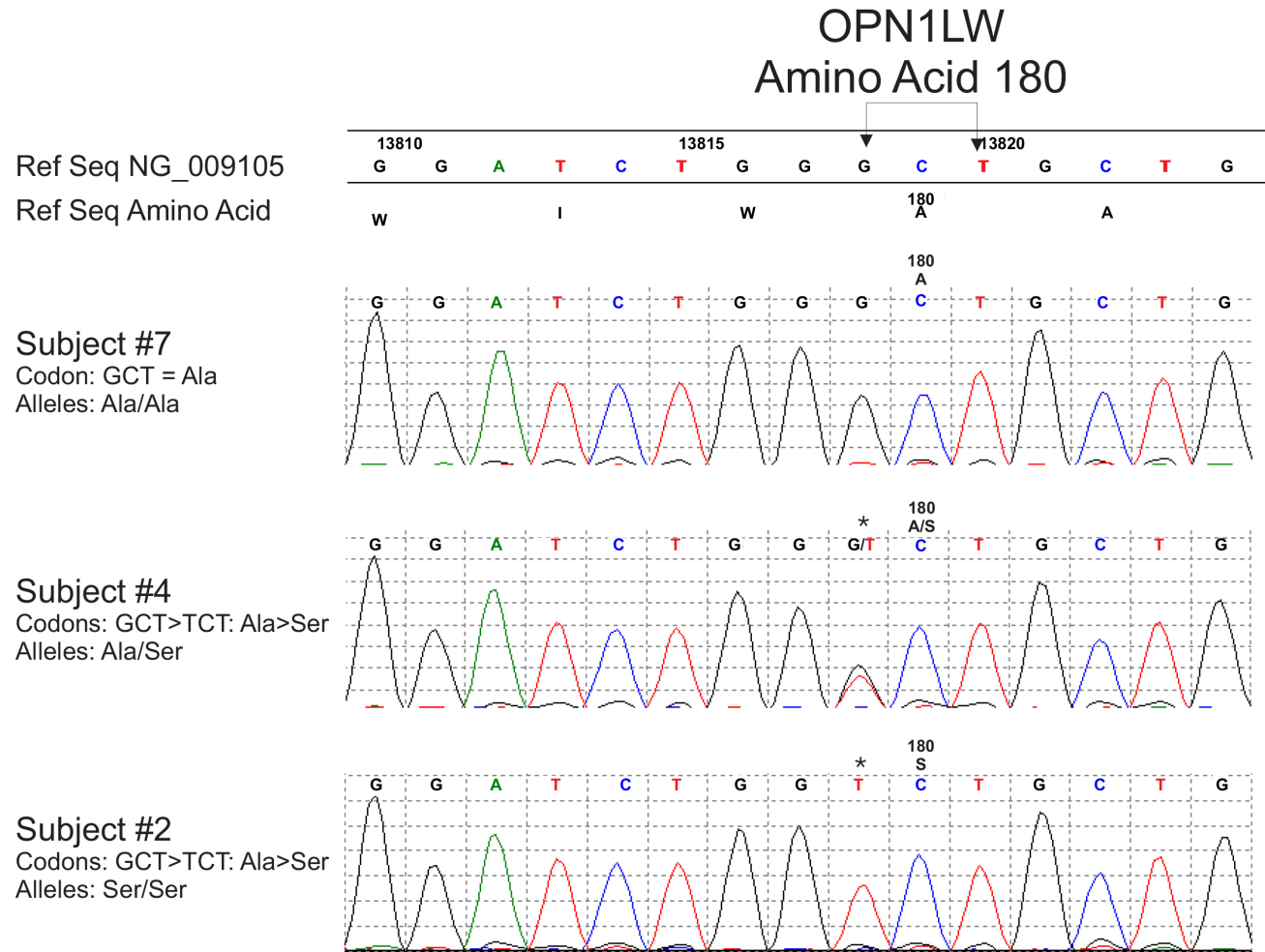
missing exon 5 of *OPN1MW*, while having a normal complement of *OPN1LW*, *OPN1SW*, and *RHO* opsin genes, would be expected to be assessed as color vision deficient, or exhibit severely anomalous perception for a subset of colors typically experienced by a trichromat with normal color vision.

As shown in Table 3, six of the nine subjects scored normal color vision on all color perception tests, measuring normal or above average performance using two standardized color vision diagnostics, the Ishihara pseudoisochromatic plates and the Farnsworth-Munsell 100 hue test, and passing the criterion for superior color vision on the ColorDx cone contrast threshold measures. Three subjects (7, 8, and 9) were assessed as low discrimination or failed the color vision assessment tests.

Therefore, we expected the photopigment opsin genotype analyses for subjects listed in Table 3 to have the following

genotype patterns: (i) Subjects 4–6 would have three gene (S-, M-, and L-opsin) trichromat genotypes (of normal or anomalous forms). (ii) Subjects 1–3 would have potential tetrachromat genotypes (S-, M-, L-, and L'-opsin) that exhibit at least one long-wavelength-sensitive photopigment heterozygosity (for example, both *OPN1LW* amino acids (serine and alanine) at codon 180 of exon 3) for female subjects with evidence of familial color deficiency. (iii) Subjects 7–9 would have two gene (e.g., S- and M-opsin, or S- and L-opsin) dichromat genotypes.

The correlations between the subjects' color vision assessments (Table 3) and the sequenced photopigment opsin genotypes (Appendix 2) were positive and consistent. Moreover, having information about a subject's opsin genotypes, even in the absence of any color vision assessment information, can provide important information on retinal processing



A. Sequence of Rhodopsin Exon 5 and Intron 5 c.36+126 including Primers, Amino Acids, and a Poly-T Region

agctggattgagtggaaggcgctggaatcgtagggggcagaagcaggcaaaagggcgaggcgaacacctactaactgcccaggtccaagcacactgtggg
F R N C M L T T I C C G K N P
cagccctggccctgactcaagcctctgtccctcag TTC CGG AAC TGC ATG CTC ACC ACC ATC TGC TGC GGC AAG AAC CCA

L G D D E A S A T V S K T E T S Q V A P A
CTG GGT GAC GAT GAG GCC TCT GCT ACC GTG TCC AAG ACG GAG ACG AGC CAG GTG GCC CCG GCC
taaga cctgctaggactctgtggccgactataggcgtctccatccctacacctcccccagccacagccatcccaccaggagcagcgcctgtgcagaatgaa
cgaagtcacataggctctctaaTTTTTTTTTTTaaagaataaataatgaggtcctcactcaccctgggacagcctgagaaggacatccaccaagacctactgac
tggagtcaccaagttcccaaggccagcgggatgtgtgcccctcctcctcccaactcatctttcaggaaacagaggattctgtttctgaaaagtgctccagcttag
ggataagtgcttagcacagaatggggcacacagtagg

Shaded regions are Exon 5 Forward and Reverse Primers

B. Description of Poly-T Regions in Subjects #1- #9

Subject	Length of Poly-T in IVS5 c.36+126
1	16
2	15
3	14
4	16
5	15
6	16
7	16
8	16
9	15

C. Phylogenetic Tree of Primates and the number of Poly T's found in Rhodopsin Intron 5 (c.36+126) (Modified from www.tolweb.org)



Figure 4. Schematic showing nucleotide sequences and amino acid profiles of the rhodopsin exon 5 and intron 5 c.36+126. **A:** Schematic showing nucleotide sequences and amino acid profiles of the rhodopsin exon 5 and intron 5 c.36+126. Amino acids are represented by capital letters. Gray highlights represent primer sites. The poly-T region is shown in red. Reference sequence is [NG_009115.1](#). **B:** The poly-T region is present in the nine subjects and ranges from 14 to 16 T nucleotides. **C:** Schematic of the primate phylogenetic tree (data from Tolweb.org) showing the poly-T repeats are highly conserved in New World monkeys, Old World monkeys, great apes, gibbons, and humans.

features (e.g., optical pigment density) that follow phenotypically from identified genotypes.

LR-PCR-Seq correlation: Spectral sensitivity and X-chromosome *OPN1MW* and *OPN1LW* genes: Spectral sensitivity response curves of normal L- and M-opsin photopigments (LWS and MWS, respectively) overlap significantly but are well separated (by “ λ -max” peak responses separated by approximately 30 nm). Amino acid dimorphisms on exon 5 at positions 277 and 285 influence the spectral differences observed between the LWS and MWS pigments. Exon 5 amino acid sequence information determines the identity of a gene as being M- class or L- class [37]. Whereas exon 3 at position 180 of both genes often contains serine or alanine, with the presence of serine producing longer peak wavelength sensitivity, and thus, is frequently investigated empirically for its impact on perceptual processing [25,36,38-40].

Because the methods presented here permit assessment of amino acid sequence variation for many loci in the opsin genotype, it can be used for a focused study of important relationships between, for example, the “three-site” composition (A180S, Y277F, and T285A) for the L- opsin and M- opsin subtypes and the expected consequences for the phenotype λ -max (nm) variation [14]. Below, we present these “three sites” for the *OPN1LW* gene and determined the expected λ -max for each subject in this study (Table 4). Subjects 1, 3, 4, and 6 had an expected wavelength range of 555–560 nm due to their amino acid heterozygosity at codon 180. Subject 2 had a predicted wavelength of 560 nm primarily from codon 180S. Subjects 5 and 7 had the amino acids 180A, Y277, and T285, and thus, the predicted wavelength was 555 nm. Only subject 8 was expected to have a 532 nm λ -max because of the A180, 277F, and 285A codon changes. The region coding for the 180 codon was absent in subject 9, and because only

the 277 and 285 codons could be determined, the predicted λ -max is unknown.

Table 4 shows that subjects 1 through 7 had stable wild-type codons for the *OPN1MW* gene that would yield the expected 532 nm λ -max. Codon 180 for subject 8 could not be sequenced; thus, the expected λ -max is unknown. In subject 9, codon 180 showed nucleotide changes that would yield A/S codon at that location. Therefore, the expected λ -max would range from 532 to 534 nm.

DISCUSSION

OPN1LW and *OPN1MW* genes:

Exons 3 and 4—Conventional PCR methods that amplify through the codon 180 region cannot distinguish between the DNA sequences of *OPN1LW* and *OPN1MW* genes due to their high sequence homology (96%). The only significant region of sequence divergence between the two genes occurs in exon 5, which is more than 3,000 bases upstream from the polymorphic region in exon 3. Jameson et al. reported genotyping methods for codon 180 dimorphisms demonstrating three possible genotypes in female subjects: Ser/Ser, Ser/Ala, and Ala/Ala [25,38]. For women who are Ser/Ala, it was not possible to determine which amino acid was specific to the *OPN1LW* and *OPN1MW* genes. Nevertheless, even with this restricted classification system, it was demonstrated that the “heterozygous” genotype individuals who have serine and alanine (i.e., Ser/Ala) possessed more diverse color perception behaviors than either homozygous genotype (i.e., Ser/Ser or Ala/Ala). The Jameson technique used four PCR steps per subject, along with multiple gels, and restriction enzymes digestion, all of which increased the potential for errors.

TABLE 4. L-OPSIN SUBTYPES IN SUBJECTS DISTINGUISHED ON THE BASIS OF ‘THREE-SITES’ COMPOSITION.

Subjects	L-Opsin: Expected λ_{\max} (nm)	L-Opsin: A180S	L-Opsin: Y277F	L-Opsin: T285A	M-Opsin: Expected λ_{\max} (nm)	M-Opsin: A180S	M-Opsin: F277Y	M-Opsin: A285T
1	555–560	A/S	Y	T	532	A	F	A
2	560	S	Y	T	532	A	F	A
3	555–560	A/S	Y	T	532	A	F	A
4	555–560	A/S	Y	T	532	A	F	A
5	555	A	Y	T	532	A	F	A
6	555–560	A/S	Y	T	532	A	F	A
7	555	A	Y	T	532	A	F	A
8	532	A	F	A	unknown	N/A	Y	T
9	unknown	N/A	F	A	532–534	A/S	F	A

N/A, not available Assignment of expected λ_{\max} (nm) based upon Kawamura et al., 2016 [14].

In comparison, the LR-PCR-Seq has the advantage of generating *OPNILW* and *OPNIMW* gene-specific PCR products employing a single PCR reaction per gene. This eliminates multiple PCR reactions per subject, saving time and money, and reducing potential errors in genotyping. In addition, the LR-PCR products, when sequenced, give more definitive results than restriction enzyme digests. The LR-PCR-Seq method uses (a) PCR primers specifically designed to extend the length of PCR-amplified DNA to more than 4,000 bp and (b) sequences the product using multiple internal sequencing primers specific for either exon 3 or exon 4.

The LR-PCR-Seq method enables accurate genotyping of not only the codon 180 polymorphism on each photopigment opsin gene but also other polymorphisms and intronic sequences, which can provide results that help predict and interpret color perception behavior. For example, sequencing of subject 8 for codons 180, 277, and 285 in *OPNILW* revealed a pattern that moved the expected λ -max from 555 to 560 nm (seen in subjects 1 through 7) to 532 nm, which was consistent with the poor performance on the FM100 test.

Exon 5—Exon 5 of *OPNILW* and exon 5 of *OPNIMW* have enough DNA sequence variability from each other to provide a location for unique reverse PCR primer annealing (Table 2) thus allowing the amplification of separate *OPNILW* and *OPNIMW* PCR products. To determine the sequence of exon 5, *OPNILW* and *OPNIMW* products were coamplified leading to a mixed PCR product and thus a mixed or heterozygous sequence. In some cases, such as subject 8 or 9, there were mutations in exon 5 that prohibited the PCR of the *OPNILW* or *OPNIMW* gene products (4,045 bp). Then the exon 5 PCR product (398 bp) sequencing could indicate which gene (*OPNILW* or *OPNIMW*) was mutated, and this could correlate to color vision performance. Subject 8 had the amino acid pattern 274V>I (15,890 G>A), 277F>Y (15,900 T>A), 279F>V (15,905 T>G), 285A>T (15,923 G>A), 298p>A (15,962 C>G), 309F>Y (15,996 T>A) which is an *OPNILW* pattern from sequencing exon 5, while subject 9 had the pattern 274I>V (17,119 A>G), 277Y>F (17,129 A>T), 279V>F (17,134 G>T), 285T>A (17,152 A>G), 298 A>P (17,191G>A), 309 Y>F (17,225 A>T; an *OPNIMW* pattern; Appendix 2). Both subjects had color vision deficiency and failed PCR reactions for either the *OPNILW* or *OPNIMW* gene, which was identified with exon 5 sequencing. This relatively simple combination of the LR-PCR-Seq of *OPNILW* or *OPNIMW* products and exon 5 products is a powerful tool that allows identification of these opsin gene deficiencies.

OPNISW gene: In the human retina, the short opsin responds to peak wavelengths for 420–440 nm and has more amino

acid homology to rhodopsin (75%) than either long or medium opsins (43%) [41]. Tritanopia is caused by genetic mutations in the short opsin exon 3 (5235G>A; Gly79Arg), exon 3 (6246T>G; Ser214Pro), and exon 4 (7005C>T; Pro264Ser). The LR-PCR-Seq method permitted genotyping of these SNPs, all of which were normal in the nine subjects we evaluated. In lower vertebrates, there are two classes of *OPNISW* opsins: class 1 that responds to 360 nm of ultraviolet-sensitive light, and class 2 that responds to 400–470 nm wavelengths [42]. Many non-primate mammals have retained dichromatic vision with the L and S opsins. Furthermore, it has been reported that in some mammals, the *OPNISW* and *OPNILW* opsins can be expressed in the same cone cell [43–45].

RHO gene: The LR-PCR-Seq of the *rhodopsin* gene yielded unremarkable sequencing results for the exons. However, a previously unreported conserved region of poly-T located within intron 5 (c.36+126), a non-coding region, was identified. When poly-T regions are present within a genome, sequencing “slippage” can occur due to loss of the T nucleotide anchor thus leading to erroneous base pair matching. The consequence of having the poly-T region in intron 5 is that the forward and reverse primers yield clean and reliable sequencing until the poly-T region. Interestingly, the poly-T region is conserved within the intronic region of the primate rhodopsin genome with the values ranging from a low of ten poly-T sites in pygmy chimpanzees to six species having 15–16 poly-T sites in the region (Figure 4C).

The functional importance of the poly-T regions is not known at this time, but a recent investigation suggested that poly-T or poly-A regions occur in the absence of DNA mismatch repair and are associated with increased mutation frequency [46]. In yeast, the poly-T/poly-A stretches affect the binding of nucleosomes within the promoter region, thus possibly contributing to translational regulation [47]. This was supported in a study showing decreased translational activity when the *ATPIA1* (Gene ID: 476 OMIM: 182310) promoter contained 12 T-insertion [48]. Johnson and coworkers showed that poly(dA:dT)-rich stretches exclude nucleosome attachment but enhance DNA looping [49]. The role of poly-T stretches in opsins is not clear and requires additional investigation.

The expected wavelength ranges based upon the “three sites” patterns were evaluated for the *OPNILW* gene in Table 4. However, the color vision and sensitivity assessments are not completely reliable methods for detecting the peak spectral response or “ λ -max” value of expressed photopigments. According to Neitz et al. (2011), spectral tuning of peak response or λ -max of human L and M cone photopigments in the phenotype follows from allelic variation in the amino

acids occurring at specific positions on exons 2 through 5 of the opsin gene. In particular, seven sites of importance for λ -max tuning occur at positions 116 on exon 2; 180 on exon 3; 230 and 233 on exon 4; and 277, 285, and 309 on exon 5. SNPs at these positions produce shifts in spectral sensitivity of the expressed pigment which additively combine to influence photoreceptor responsivity in the expressed phenotype [1,37]. Other early visual processing factors additionally impact spectral tuning of λ -max, such as macular pigment and photopigment optical density and preretinal filtering. The consequences of these additional factors are important when modeling an individual's expressed retinal photopigment phenotype. Photopigment variations resulting from allelic opsin gene sequences have been found to correlate largely, but not absolutely, with phenotypes established with color vision testing. Further research is needed to refine the assessment of photopigment opsin genotyping using perceptual measures [50].

Recent advances in adaptive optics technologies provide important tools for visualization of functioning photopigment classes in the mosaics in the living human retina [51,52]. The variations in the structure of an individual's expressed cone mosaic are expected to influence visual perception function. In the present investigation, we did not assess these features of the participants' expressed cone mosaics, partly because differentiation of many X-linked photopigment variants remains difficult, as measuring in vivo the spectral response properties of different photopigments with similar spectral response functions remains technically challenging. Moreover, the collection of data is complicated by several varying factors for each individual, such as photopigment spectral-peak response proximity, varying optical density of pigments, variation in cell "wave-guiding" morphology, and ocular media filtering. Nevertheless, because variations in color vision phenotypes depend on opsin genotype sequences as an initial defining limiting condition, the use of individual opsin-genotype data to investigate behaviors associated is an important first step in characterizing variations in color vision phenotypes.

Summary: There is increased interest in correlating the clinical color phenotypes with the subject's genotype in disease processes, understanding color processing and classifications of color deficiencies. Major advantages of the LR-PCR-Seq technique are that it (a) provides a uniform platform that can be applied to all the opsin genes known to be instrumental for color vision and perception of light at photopic and scotopic levels; (b) entire exon and intron regions can be analyzed, which may allow classification of SNP or codon variations that account for rare color vision gene defects; (c) the

procedure can identify deletions from opsin genes that previously have been missed because the methods used amplification of short, focused PCR products rather than the entire opsin gene; (d) the predicted maximum kilobase pairs that the FailSafe PCR system can amplify is up to 20 kb and the actual maximum kilobase pairs our laboratory has successfully amplified and sequenced is 11.5 kb [53] and (e) the costs for analyzing subjects are reduced because only a single large PCR reaction per gene and sequencing is required.

The current limitations of the LR-PCR-Seq method are the following: (a) Exon 5 of *OPN1LW* and exon 5 of *OPN1MW* cannot be separately PCR amplified or sequenced, but the combined sequences can be determined by this method, which provides insight into whether this important exon has both sequences or one. (b) Exon 1 of *OPN1LW* and exon 1 of *OPN1MW* are not amplified or sequenced. (c) Exon 6 of *OPN1MW* is not amplified or sequenced. Our laboratory is currently working on extending LR-PCR Seq to include *OPN1LW* and *OPN1MW* exons 1 and 6 and to separate out exon 5.

The present LR-PCR-Seq methodology offers a reliable, cost-effective method for identifying SNP changes within the various opsin genes. However, regulation of the opsin genes also involves the status of cytosine methylation of the *OPN1LW* and *OPN1MW* promoters [54]. Deeb et al. performed a series of elegant experiments using one cell line (WERI-Rb1 cells) that expresses the L- or M- pigment mRNA when cultured in the presence of thyroid hormone receptor β 2 while a second lymphoblastoid cell line does not produce the L- or M- pigments. Analyses of the methylated cytosine in the CpG dinucleotides in the WERI-Rb1 cells showed hypomethylation of the promoters for L-opsin and M-opsin genes along with the upstream DNaseI-hypersensitive (DHS) site. In contrast, the lymphoblastoid cell line was highly methylated in those regions, which would lead to chromatin condensation and silencing expression of the L- and M-opsin genes. Merbs et al. used bisulfite sequencing to demonstrate differential methylation patterns that correlated inversely to the expression of each of the opsin genes (*RHO*, *OPN1LW*, *OPN1MW*, and *OPN1SW*) suggesting that epigenetic regulation plays a role in photoreceptor development [55]. More recently, it was shown that inhibition of histone deacetylases (HDACs) modulated the cell cycle of differentiating retinal progenitor cells and decreased rhodopsin levels [56]. Finally, it has been shown that mechanisms of epigenetic gene-silencing, involving the *Samd7* gene, play a role in rod photoreceptor development and function [57]. To more fully understand regulation of opsin genes, a combined approach of DNA sequencing, along with epigenetic analyses should be

conducted for individuals with normal color vision and color vision deficiency.

APPENDIX 1. TABLE OF SEQUENCING RESULTS.

To access the data, click or select the words “[Appendix 1.](#)”

APPENDIX 2. OPN1LW, OPN1MW, OPN1SW AND RHO SNPS IDENTIFIED BY LR-PCR-SEQ.

To access the data, click or select the words “[Appendix 2.](#)” Minor allele frequency (MAF): MAF is the frequency of the minor allele. MAF is often reported in the context of allele frequencies established by the 1000 Genomes and other large sequencing projects. When there are more than two alleles, MAF refers to the second most frequent allele. N/A: No frequency data noted in NCBI dbSNP data base.

ACKNOWLEDGMENTS

This work was funded in part by the National Science Foundation awards (SMA-1416907, Jameson PI; SES-0724228, Jameson Co-PI; SBE-9973903, Jameson PI; IOS-1656260, Briscoe PI). A Hellman Faculty Fellowship Award 1997 (Jameson); UCI SOM/Ayala BioSci Pilot Funding Award (Jameson, Briscoe and Kenney); Discovery Eye Foundation (Kenney), and unrestricted grant from Research to Prevent Blindness (Kenney). Views and opinions expressed in this work are those of the authors and do not necessarily reflect the official policy or position of any agency of the University of California, the Discovery Eye Foundation or the National Science Foundation. We thank the subjects who participated in this study.

REFERENCES

- Asenjo AB, Rim J, Oprian DD. Molecular determinants of human red/green color discrimination. *Neuron* 1994; 12:1131-8. [PMID: 8185948].
- Merbs SL, Nathans J. Absorption spectra of human cone pigments. *Nature* 1992; 356:433-5. [PMID: 1557124].
- Merbs SL, Nathans J. Absorption spectra of the hybrid pigments responsible for anomalous color vision. *Science* 1992; 258:464-6. [PMID: 1411542].
- Merbs SL, Nathans J. Role of hydroxyl-bearing amino acids in differentially tuning the absorption spectra of the human red and green cone pigments. *Photochem Photobiol* 1993; 58:706-10. [PMID: 8284327].
- Neitz M, Neitz J, Jacobs GH. Spectral tuning of pigments underlying red-green color vision. *Science* 1991; 252:971-4. [PMID: 1903559].
- Winderickx J, Lindsey DT, Sanocki E, Teller DY, Motulsky AG, Deeb SS. Polymorphism in red photopigment underlies variation in colour matching. *Nature* 1992; 356:431-3. [PMID: 1557123].
- Neitz M, Neitz J, Jacobs GH. Genetic basis of photopigment variations in human dichromats. *Vision Res* 1995; 35:2095-103. [PMID: 7667922].
- Hofer H, Singer B, Williams DR. Different sensations from cones with the same photopigment. *J Vis* 2005; 5:444-54. [PMID: 16097875].
- Brainard DH, Williams DR, Hofer H. Trichromatic reconstruction from the interleaved cone mosaic: Bayesian model and the color appearance of small spots. *J Vis* 2008; 8:1-23. .
- Deeb SS. Molecular genetics of colour vision deficiencies. *Clin Exp Optom* 2004; 87:224-9. [PMID: 15312026].
- Shyue SK, Boissinot S, Schneider H, Sampaio I, Schneider MP, Abee CR, Williams L, Hewett-Emmett D, Sperling HG, Cowing JA, Dulai KS, Hunt DM, Li WH. Molecular genetics of spectral tuning in New World monkey color vision. *J Mol Evol* 1998; 46:697-702. [PMID: 9608052].
- Yokoyama S, Radlwimmer FB. The molecular genetics of red and green color vision in mammals. *Genetics* 1999; 153:919-32. [PMID: 10511567].
- Zhao Z, Hewett-Emmett D, Li WH. Frequent gene conversion between human red and green opsin genes. *J Mol Evol* 1998; 46:494-6. [PMID: 9541545].
- Kawamura S. Color vision diversity and significance in primates inferred from genetic and field studies. *Genes Genomics* 2016; 38:779-91. [PMID: 27594978].
- Neitz M, Carroll J, Renner A, Knau H, Werner JS, Neitz J. Variety of genotypes in males diagnosed as dichromatic on a conventional clinical anomaloscope. *Vis Neurosci* 2004; 21:205-16. [PMID: 15518190].
- Carroll J, Dubra A, Gardner JC, Mizrahi-Meissonnier L, Cooper RF, Dubis AM, Nordgren R, Genead M, Connor TB Jr, Stepien KE, Sharon D, Hunt DM, Banin E, Hardcastle AJ, Moore AT, Williams DR, Fishman G, Neitz J, Neitz M, Michaelides M. The effect of cone opsin mutations on retinal structure and the integrity of the photoreceptor mosaic. *Invest Ophthalmol Vis Sci* 2012; 53:8006-15. [PMID: 23139274].
- Gardner JC, Liew G, Quan Y, Ermetal B, Ueyama H, Davidson AE, Schwarz N, Kanuga N, Chana R, Maher ER, Webster AR, Holder GE, Robson AG, Cheetham ME, Liebelt J, Ruddle JB, Moore AT, Michaelides M, Hardcastle AJ. Three different cone opsin gene array mutational mechanisms with genotype-phenotype correlation and functional investigation of cone opsin variants. *Hum Mutat* 2014; 35:1354-62. [PMID: 25168334].
- Michaelides M, Johnson S, Simunovic MP, Bradshaw K, Holder G, Mollon JD, Moore AT, Hunt DM. Blue cone monochromatism: a phenotype and genotype assessment with evidence of progressive loss of cone function in older individuals. *Eye (Lond)* 2005; 19:2-10. [PMID: 15094734].
- Gardner JC, Michaelides M, Holder GE, Kanuga N, Webb TR, Mollon JD, Moore AT, Hardcastle AJ. Blue cone

- monochromacy: causative mutations and associated phenotypes. *Mol Vis* 2009; 15:876-84. [PMID: 19421413].
20. Oda S, Ueyama H, Nishida Y, Tanabe S, Yamade S. Analysis of L-cone/M-cone visual pigment gene arrays in females by long-range PCR. *Vision Res* 2003; 43:489-95. [PMID: 12594995].
 21. de Albuquerque DM, Costa SC. Genotyping of human cytomegalovirus using non-radioactive single-strand conformation polymorphism (SSCP) analysis. *J Virol Methods* 2003; 110:25-8. [PMID: 12757917].
 22. Xu WX, Hong N, Zhang JK, Wang GP. Improving the sensitivity of single-strand conformation polymorphism (SSCP) to study the variability of PLMVd. *J Virol Methods* 2006; 135:276-80. [PMID: 16644025].
 23. Elleuch A, Hamdi I, Bessaies N, Fakhfakj H. Single-strand conformation polymorphism for molecular variability studies of six viroid species. *Biosci Biotechnol Biochem* 2013; 77:182-8. [PMID: 23291763].
 24. Pajak B, Lepek K. Native nucleic acid electrophoresis as an efficient alternative for genotyping method of influenza virus. *Acta Biochim Pol* 2014; 61:479-83. [PMID: 25180222].
 25. Jameson KA, Highnote SM, Wasserman LM. Richer color experience in observers with multiple photopigment opsin genes. *Psychon Bull Rev* 2001; 8:244-61. [PMID: 11495112].
 26. Wasserman LM, Szeszel MK, Jameson KA. Long-range polymerase chain reaction analysis for specifying photopigment opsin gene polymorphisms. Technical Report Series #MBS 09-07. Institute for Mathematical Behavioral Sciences. 2009.
 27. Davidoff C, Neitz M, Neitz J. Genetic testing as a new standard for clinical diagnosis of color vision deficiencies. *Transl Vis Sci Technol* 2016; 5:2-[PMID: 27622081].
 28. Mytelka DS, Chamberlin MJ. Analysis and suppression of DNA polymerase pauses associated with a trinucleotide consensus. *Nucleic Acids Res* 1996; 24:2774-81. [PMID: 8759010].
 29. Henke W, Kerdel K, Jung K, Schnorr D, Loening SA. Betaine improves the PCR amplification of GC-rich DNA sequences. *Nucleic Acids Res* 1997; 25:3957-8. [PMID: 9380524].
 30. Weissensteiner T, Lanchbury JS. Strategy for controlling preferential amplification and avoiding false negatives in PCR typing. *Biotechniques* 1996; 21:1102-8. [PMID: 8969839].
 31. Farnsworth D. The Farnsworth-Munsell 100-hue test: For the examination of color discrimination Manual. 1957, Baltimore: Macbeth.
 32. Clark JH. The Ishihara test for color blindness. *American Journal of Physiological Optics* 1924; 5:269-76. .
 33. Fujikawa M, Mraki S, Niwa Y, Ohji M. Evaluation of clinical validity of the Rabin cone contrast test in normal phakic or pseudophakic eyes and severely dichromatic eyes. *Acta Ophthalmol* 2018; 96:e164-7. [PMID: 28556475].
 34. Niwa Y, Muraki S, Naito F, Minamikawa T, Ohji M. Evaluation of acquired color vision deficiency in glaucoma using the Rabin cone contrast test. *Invest Ophthalmol Vis Sci* 2014; 55:6686-90. [PMID: 25168899].
 35. Prins N. The psi-marginal adaptive method: How to give nuisance parameters the attention they deserve (no more, no less). *J Vis* 2013; 13:3-[PMID: 23750016].
 36. Deeb SS. The molecular basis of variation in human color vision. *Clin Genet* 2005; 67:369-77. [PMID: 15811001].
 37. Neitz J, Neitz M. The genetics of normal and defective color vision. *Vision Res* 2011; 51:633-51. [PMID: 21167193].
 38. Jameson KA, Bimler D, Wasserman LM. Re-assessing perceptual diagnostics for observers with diverse retinal photopigments genotypes. *Progress i Colour Studies 2: Cognition*, ed. N.J. Pitchford, Bigga, C. P. 2006: John Benjamins. 13-33.
 39. Jordan G, Deeb SS, Bosten JM, Mollon JD. The dimensionality of color vision in carriers of anomalous trichromacy. *J Vis* 2010; 10:12-[PMID: 20884587].
 40. Bochko V, Jameson KA. Investigating potential human tetrachromacy in individuals with tetrachromat genotypes using multispectral techniques. *Electronic imaging, human vision and electronic imaging (12)*. Society for Imaging Science and Technology., 2018: p. 1-12.
 41. Nathans J, Thomas D, Hogness DS. Molecular genetics of human color vision: the genes encoding blue, green, and red pigments. *Science* 1986; 232:193-202. [PMID: 2937147].
 42. Hunt DM, Peichl L. S cones: Evolution, retinal distribution, development, and spectral sensitivity. *Vis Neurosci* 2014; 31:115-38. [PMID: 23895771].
 43. Rohlich P, van Veen T, Szel A. Two different visual pigments in one retinal cone cell. *Neuron* 1994; 13:1159-66. [PMID: 7946352].
 44. Szel A, Rohlich P, Caffé AR, van Veen T. Distribution of cone photoreceptors in the mammalian retina. *Microsc Res Tech* 1996; 35:445-62. [PMID: 9016448].
 45. Lukats A, Szabo A, Rohlich P, Vigh B. Photopigment coexpression in mammals: comparative and developmental aspects. *Histol Histopathol* 2005; 20:551-74. [PMID: 15736061].
 46. Belfield EJ, Ding ZJ, Jamieson FJC, Visscher AM, Zheng SJ, Mithani A, Harberd NP. DNA mismatch repair preferentially protects genes from mutation. *Genome Res* 2018; 28:66-74. [PMID: 29233924].
 47. de Boer CG, Hughes TR. Poly-dA:dT tracts form an in vivo nucleosomal turnstile. *PLoS One* 2014; 9:e110479-[PMID: 25353956].
 48. Herrera VL, Pasion KA, Moran AM, Zaninello R, Ortu MF, Fresu G, Piras DA, Argiolas G, Troffa C, Glorioso V, Masala W, Glorioso N, Ruiz-Opazo N. A functional 12T-insertion polymorphism in the ATP1A1 promoter confers decreased susceptibility to hypertension in a male Sardinian population. *PLoS One* 2015; 10:e0116724-[PMID: 25615575].
 49. Johnson S, Chen YJ, Phillips R. Poly(dA:dT)-rich DNAs are highly flexible in the context of DNA looping. *PLoS One* 2013; 8:e75799-[PMID: 24146776].

50. Jameson KA, Joe KC, Bochko VA, Satalich TA, Atilano SR, Kenney MC. Human color vision and tetrachromacy. Elements in Perception. Vol. In Press. 2019, Cambridge: Cambridge University Press.
51. Carroll J, Gray DC, Roorda A, Williams DR. Recent advances in retinal imaging with Percher optics. Opt Photonics News 2005; 16:36-42. .
52. Pircher M, Zawadzki RJ. Review of adaptive optics OCT (AO-OCT): principles and applications for retinal imaging Biomed Opt Express 2017; 8:2536-62. Invited[PMID: 28663890].
53. Kenney MC, Chwa M, Atilano SR, Falatoonzadeh P, Ramirez C, Malik D, Tarek M, Caceres-del-Carpio J, Nesburn AB, Boyer DS, Kuppermann BD, Vawter M, Jazwinski SM, Miceli M, Wallace DC, Udar N. Inherited mitochondrial DNA variants can affect complement, inflammation, and apoptosis pathways: insights into mitochondrial-nuclear interactions. Hum Mol Genet 2014; 23:3537-3551[PMID: 24584571].
54. Deeb SS, Bisset D, Fu L. Epigenetic control of expression of the human L- and M- pigment genes. Ophthalmic Physiol Opt 2010; 30:446-53. [PMID: 20883327].
55. Merbs SL, Khan MA, Hackler L Jr, Oliver VF, Wan J, Qian J, Zack DJ. Cell-specific DNA methylation patterns of retina-specific genes. PLoS One 2012; 7:e32602-[PMID: 22403679].
56. Ferreira RC, Popova EY, James J, Briones MR, Zhang SS, Barnstable CJ. Histone deacetylase 1 is essential for rod photoreceptor differentiation by regulating acetylation at histone H3 lysine 9 and histone H4 lysine 12 in the mouse retina. J Biol Chem 2017; 292:2422-40. [PMID: 28028172].
57. Omori Y, Kubo S, Kon T, Furuhashi M, Narita H, Kominami T, Ueno A, Tsutsumi R, Chaya T, Yamamoto H, Suetake I, Ueno S, Koseki H, Nakagawa A, Furukawa T. Samd7 is a cell type-specific PRC1 component essential for establishing retinal rod photoreceptor identity. Proc Natl Acad Sci USA 2017; 114:E8264-73. [PMID: 28900001].

Articles are provided courtesy of Emory University and the Zhongshan Ophthalmic Center, Sun Yat-sen University, P.R. China. The print version of this article was created on 5 March 2020. This reflects all typographical corrections and errata to the article through that date. Details of any changes may be found in the online version of the article.